Geophysical Research Letters

RESEARCH LETTER
10.1029/2018GL079519

Key Points:
- New borehole seismic and geodetic data from the updip end of the Cascadia subduction zone show no evidence of triggered tremor or slow slip during the passage of teleseismic surface waves
- There is a clear contrast in the behavior of triggered tremor between the updip and downdip ends of the Cascadia subduction zone at Vancouver Island
- Borehole tilt can rule out slow slip events at the M_w 4.0 level

Supporting Information:
- Supporting Information S1

Correspondence to:
J. J. McGuire,
jmcguire@whoi.edu

Citation:
McGuire, J. J., Collins, J. A., Davis, E., Becker, K., & Heesemann, M. (2018). A lack of dynamic triggering of slow slip and tremor indicates that the shallow Cascadia megathrust offshore Vancouver Island is likely locked. *Geophysical Research Letters*, *45*, 11,095–11,103. https://doi.org/10.1029/2018GL079519

Received 6 JUL 2018
Accepted 8 OCT 2018
Accepted article online 12 OCT 2018
Published online 27 OCT 2018

A Lack of Dynamic Triggering of Slow Slip and Tremor Indicates That the Shallow Cascadia Megathrust Offshore Vancouver Island Is Likely Locked

Jeffrey J. McGuire[1], John A. Collins[1], Earl Davis[2], Keir Becker[3], and Martin Heesemann[4,5]

[1]Department of Geology and Geophysics, Woods Hole Oceanographic Institution, Woods Hole, MA, USA, [2]Pacific Geoscience Centre, Geological Survey of Canada, Sidney, British Columbia, Canada, [3]Department of Marine Geosciences, University of Miami–RSMAS, Miami, FL, USA, [4]Ocean Networks Canada, University of Victoria, Victoria, British Columbia, Canada, [5]School of Earth and Ocean Sciences, University of Victoria, Victoria, British Columbia, Canada

Abstract Great subduction zone earthquakes vary considerably in the updip extent of megathrust rupture. It is unclear if this diversity reflects variations in interseismic strain accumulation owing to the limited number of subduction zones with seafloor monitoring. We use a borehole seismic-geodetic observatory installed at the updip end of the Cascadia fault offshore Vancouver Island to show that the megathrust there does not appear to slip in triggered tremor or slow-slip events when subjected to moderate dynamic stress transients. Borehole tilt and seismic data from recent teleseismic *M*7.6–8.1 earthquakes demonstrate a lack of triggered slow slip above the M_w 4.0 level and an absence of triggered tremor despite shear-stress transients of 1–10 kPa that were sufficient to trigger tremor on the downdip end of the interface. Our observations are most consistent with a model in which the Cascadia fault offshore Vancouver Island is locked all the way to the trench.

Plain Language Summary Subduction zone thrust faults are generally thought to contain three primary regions in terms of earthquake rupture. Both the shallowest region near the trench (depths <~5–10 km) and the deeper onshore region (depths >~35 km) are thought to fail primarily without earthquakes, while seismic slip is contained primarily within the intervening depth range (~5–35 km). In many subduction zones around the world, the deeper region has been observed to emit small amounts of seismic radiation when nonvolcanic tremor events are triggered by passing seismic waves. Similarly, the shallowest portions of a few subduction zones behave the same way. Here we study the Cascadia subduction zone with newly available subseafloor seismic and geodetic data that indicate a clear difference in behavior between the deep and shallow parts of the fault. This likely indicates that strain is accumulated across most of the breadth of the accretionary prism and that the shallow part of the fault may rupture during great earthquakes.

1. Introduction

Great subduction zone earthquakes vary considerably in their tsunami generation because the updip extent of megathrust rupture can range from ~10 km depth (Briggs et al., 2006; Duputel et al., 2015; Sun et al., 2017) to the trench (Iinuma et al., 2012; Sun et al., 2017). It is unclear if this diversity reflects variations in interseismic strain accumulation. The limited seafloor geodetic data available show that in some locations, such as Peru, the fault is locked all the way to the trench (Gagnon et al., 2005), while in others, such as Hikurangi (New Zealand), Costa Rica, and Nankai (Japan), the updip portion regularly fails in slow-slip events (Araki et al., 2017; Davis et al., 2013, 2015; Wallace et al., 2016) with limited interseismic locking (Dixon et al., 2014; Yokota et al., 2016). The Cascadia subduction zone has a history of great earthquakes and tsunamis (Atwater, 1987; Goldfinger et al., 2012), but the extent of interseismic locking at the updip end of the megathrust is not constrained by onshore geodetic measurements (Pollitz & Evans, 2017; Schmalzle et al., 2014; Wang & Tréhu, 2016).

Recent studies of shallow subduction zone faults have demonstrated a rich set of slip events (Obara & Kato, 2016) including coseismic slip in great earthquakes (Iinuma et al., 2012; Sun, Fujiwara, et al., 2017), afterslip (Davis et al., 2015; Sun, Davis, et al., 2017), very low frequency earthquakes (VLFEs; Nakamura & Sunagawa, 2015; Obara & Ito, 2005; Walter et al., 2013), tremor (Brown et al., 2005), and slow slip events

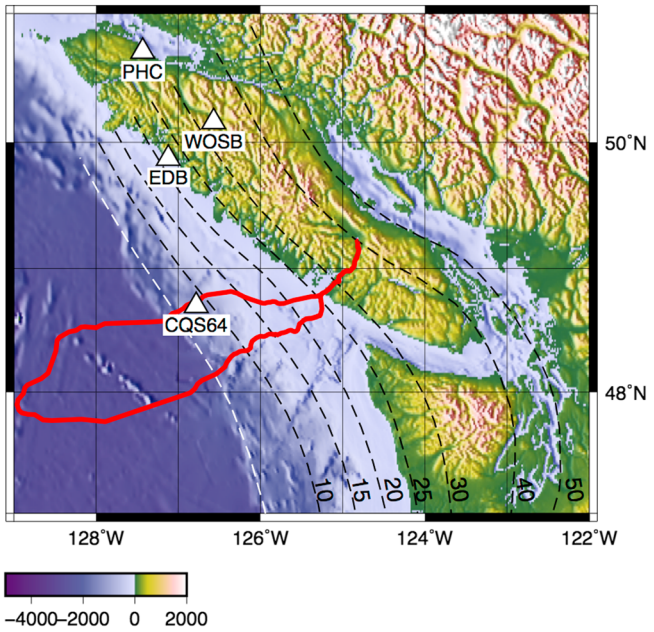

Figure 1. Map of the northern Cascadia subduction zone. The dashed black contours denote the top of the plate interface (McCrory et al., 2012; in km), and the white contour denotes the approximate location of the deformation front. The red line denotes the ONC NEPTUNE observatory cable route. The triangles denote the locations of seismic and geodetic stations in Figures 2 and 3. The Clayoquot slope borehole observatory at Integrated Ocean Drilling Program hole U1364A is located about 20 km from the deformation front where the plate interface is likely at a depth of about 5 km (Yuan et al., 1994).

(SSEs) with durations of days to weeks (Araki et al., 2017; Davis et al., 2013; Wallace et al., 2016). Perhaps the most dramatic example is the triggering of an ~300-km long, *M*7, slow-slip event in the Hikurangi subduction zone (Wallace et al., 2017) by the 2016 M_w 7.8 crustal Kaikoura earthquake 300–600 km farther south in New Zealand. Similarly, the two largest shallow SSEs recently observed in the Nankai Trough were likely triggered by the passing seismic waves from large earthquakes (Araki et al., 2017). A similar combination of spontaneous and dynamically triggered shallow SSEs is common in the upper few kilometers of crustal strike-slip faults in sedimentary basins (Bilham, 1989; Rymer et al., 2011; Wei et al., 2011, 2015). Moreover, the triggering of SSEs provides a direct constraint on the frictional properties of the shallow fault zone (Kaneko & Fialko, 2011; Wei et al., 2013, 2015, 2018), indicating that the shallowest regions of some faults relieve interseismic strain through aseismic transient creep. This updip behavior mirrors the sensitivity of subduction faults downdip of the seismogenic zone where transient stress changes routinely trigger tremor and other forms of slow slip (Miyazawa & Brodsky, 2008; Peng & Gomberg, 2010; Rubinstein et al., 2007, 2009).

Cascadia has long been recognized as an end-member example of a warm subduction zone where the prevailing mineralogy might be expected to favor co-seismic slip all the way to the trench (Hyndman & Wang, 1995), but it has been difficult to verify or reject this hypothesis with direct observations (Wang & Tréhu, 2016). Owing to the lack of resolution of interseismic coupling in the shallow portion of the fault by onshore geodetic data (Pollitz & Evans, 2017; Schmalzle et al., 2014), seafloor-based data sets are required to investigate the frictional behavior and locking state of the shallow Cascadia subduction zone.

2. Data

In 2010, the Integrated Ocean Drilling Program Expedition 328 drilled and instrumented a subseafloor hydrological observatory in hole U1364A near the updip end of the Cascadia subduction zone at a location known as Clayoquot Slope (Figure 1) to study the fluid flow and mechanical properties of the accretionary wedge (Davis et al., 2010). The hole is cased, open to a depth of 302 m below seafloor (mbsf), and sealed at the bottom with a bridge plug backed with cement. International Ocean Drilling Program installed an ACORK observatory system to allow monitoring of rock formation pressure at four screens located at 304, 244, 203, and 156 m below the seafloor. In 2016, a team from WHOI, the Univ. of Miami, and Ocean Networks Canada (ONC) installed an instrument string that was connected in summer 2017 to the ONC NEPTUNE observatory, which provides power and real-time data telemetry to shore through its cabled Clayoquot Slope Node (Figure 1). The additional instrumentation consists of a broadband seismometer and two high resolution (nanoradian) Haliburton Denali tiltmeters and two coarse resolution tiltmeters, as well as 24 thermistors. The seismometer and tiltmeters are contained within a single pressure housing that is mechanically clamped to the well casing near the bottom of the borehole (~280 mbsf), about 4.5 km above the thrust interface (Yuan et al., 1994). The thermistors are installed at regular depth intervals between the seafloor and the clamped instrument package, with a concentration around a bottom simulating reflector at a depth of ~230 mbsf. All of the data from these instruments (pressure, seismic, tilt, and temperature) are archived and made openly available via the ONC and IRIS data centers.

Since the installation of the borehole geophysical instrumentation we have recorded the seismic waves from four large distant earthquakes: the 17 July 2017 M_w 7.7 Komandorskiye Russia earthquake (4,300 km distant), the 10 January 2018 M_w 7.6 Honduras earthquake (5,200 km distant), the 8 September 2017 M_w 8.1 Chiapas Mexico earthquake (4,700 km distant), and the 23 January 2018 M_w 7.8 Gulf of Alaska earthquake (1,700 km distant). All four of these events generated large amplitude seismic surface waves (Figures 2 and S1 in the supporting information). We estimate the dynamic shear stress changes on the

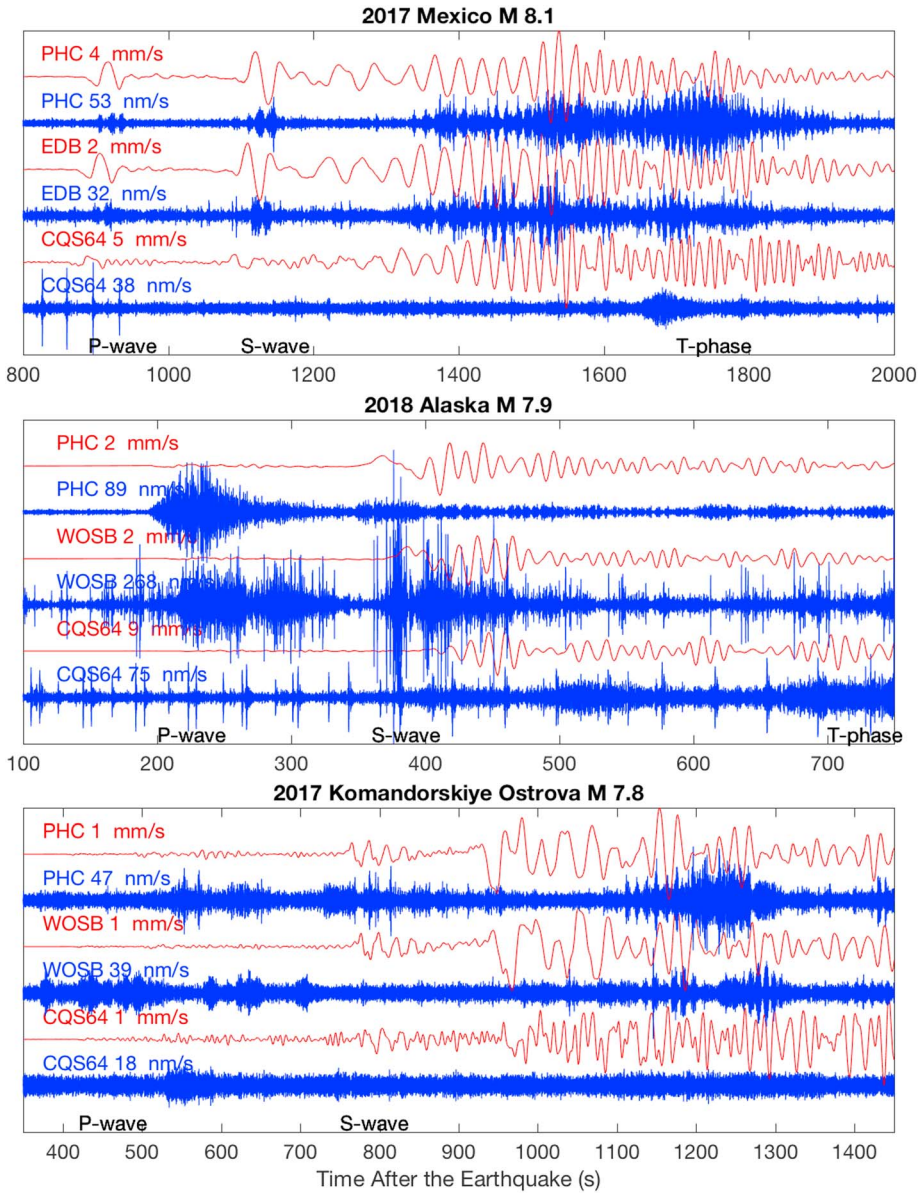

Figure 2. Examples of triggered tremor at onshore Vancouver Island seismic stations (PHC, EDB, WOSB) near the downdip edge of the locked zone and the lack of triggered tremor offshore observed in the borehole station (CQS64) near the updip end of the locked zone (see Figure 1). For each station, seismograms are shown with a high-frequency bandpass filter (blue, 8–18 Hz) and a low-frequency bandpass filter (red, 0.005 to 0.2 Hz) during the body and surface wave arrival time period. The components were chosen to highlight the triggered tremor. For all three earthquakes, the low-frequency seismogram is the horizontal velocity oriented in the updip direction (235°). For Alaska and Komandorskiye, the high-frequency waveform is the vertical component, while for the Mexico earthquake, the high-frequency seismogram is the updip direction. There are T-phase arrivals from earthquakes on the Juan de Fuca plate at 1,700 s in the top panel and ~700 s in the middle panel that were verified as T-phases by their appearance at multiple stations of the ONC network including station 1027 far from the subduction zone. Each velocity seismogram is labeled with its peak amplitude. The periodic signals on CQS64 are fin whale calls that are part of a sequence that began well before the earthquake.

thrust interface from the broadband seismic data following Cattania et al. (2017). To convert the strain tensor at depth to a stress tensor, we assumed a Poisson solid with a shear modulus of 9 GPa that is derived from compliance inversions for *S* wave speed in the accretionary wedge (2.0 km/s average; Collins et al., 2013) and a density of 2.25 g/cm^3 corresponding to an average porosity of about 0.25 (Hyndman et al., 1993). The Gulf of Alaska and Chiapas earthquakes produced shear stress variations in

the 5- to 10-kPa range, while the Honduras and Komandorskiye earthquakes were in the 1-kPa range. Dynamic stress changes of this magnitude are often interpreted to trigger downdip tremor and low-frequency earthquakes (Miyazawa & Brodsky, 2008; Rubinstein et al., 2007). The magnitude of stress change required to trigger SSEs is less clear due to fewer observations, but stress changes ranging from 0.6 to 600 kPa have triggered SSEs in subduction zones including New Zealand (Wallace et al., 2017; Wei et al., 2018), Japan (Araki et al., 2017; Itaba & Ando, 2011), and Mexico (Zigone et al., 2012). Thus, the plate interface beneath our borehole observatory has been subjected to dynamic stress changes sufficient to trigger tremor and SSEs in other subduction zones.

3. Results

We use the Komandorskiye, Mexico, and Gulf of Alaska earthquakes to look for triggered updip tremor, and the Mexico, Honduras, and Gulf of Alaska earthquakes to look for triggered slow slip in response to these transient forcings. The Honduras earthquake was excluded from the tremor study due to high whale activity (Wilcock et al., 2014) on that day, and the Komandorskiye earthquake was excluded from searching for SSEs because it occurred shortly (2 days) after the system was powered on and the tiltmeters were still reaching a stable state.

To search for updip triggered tremor in Cascadia we investigated the low-noise borehole seismograms from each large earthquake. Figure 2 shows the low-frequency surface wave arrivals from distant earthquakes and the high-frequency response from local faults. The surface waves from these earthquakes were sufficiently large to trigger seismic tremor on the deeper part of the thrust interface (~30 km) downdip of the seismogenic zone (Figure 2), which is a common observation on Vancouver Island seismic stations (Rubinstein et al., 2009). However, similar stress perturbations did not trigger any tremor on the updip portion of the same fault (Figure 2). The high frequency noise levels on the borehole seismometer are low even for the horizontal channels and are below the levels seen at coastal onshore stations (Figure 2). Thus, we would be able to observe shallow tremor if it had been triggered by any of these earthquakes.

Figure 2 shows that for the Mexico earthquake, the onshore sites PHC and EDB show clear tremor bursts occurring during peaks of the low frequency surface waves similar to previous studies. Conversely, the CQS64 borehole record shows no triggered tremor despite small noise levels. The Alaska earthquake shows similar beating of triggered tremor at PHC while WHC is noisy, and there is no clear tremor at CQS64 albeit with higher noise levels. For the Komandorskiye earthquake, triggered tremor is visible on PHC and WOSB but not CQS64 despite low noise levels. To calculate the associated stress changes (Figure S1), we estimated the orientation of the borehole seismometer channels as LH2 = 315° (east of north) and LH1 = 225° by comparing data from the borehole seismometer with data from the nearby (<5 km) oriented station NC89 and with low frequency synthetic seismograms (Tromp et al., 2010) for a number of earthquakes.

In other subduction zones, including Costa Rica (Brown et al., 2005) and Nankai (Araki et al., 2017; Nakano et al., 2018), updip tremor has been observed in the ~1- to 10-Hz band and is often contemporaneous with slow slip, VLFEs and fluid-flow transients. Moreover, both 1- to 10-Hz tremor and SSEs are dynamically triggered by passing surface waves in Nankai (Araki et al., 2017; To et al., 2015). Similarly, the downdip part of the subduction zone beneath Vancouver Island shows triggered tremor that beats with the surface wave polarity, while the updip region recorded in the borehole shows no evidence for triggered tremor (Figure 2). The lack of triggered tremor contrasts with other subduction zones, where similar amplitude surface waves trigger shallow SSEs (Araki et al., 2017; Nakano et al., 2018). Figure 2 shows that this type of triggered fault slip, which is common in Nankai and is associated with high pore fluid pressures, did not occur on the updip end of Cascadia offshore of Vancouver Island. Since triggered tremor and VLFEs sometimes bracket the seismogenic portion of subduction thrust faults (Nakamura & Sunagawa, 2015), the lack of tremor indicates the updip region near the Clayoquot Slope borehole observatory is likely locked during the current interseismic period.

To determine if there were any SSEs triggered by the passing surface waves, we first removed the tidal signal from the tilt data using the BAYTAP08 Bayesian modeling procedure (Tamura et al., 1991; https://igppweb.ucsd.edu/~agnew/Baytap/baytap.html). BAYTAP08 estimates tidal amplitude and phase for a set of known tidal constituents using the Akaike Bayesian information criterion as a goodness-of-fit measure, and in addition determines a smoothness-constrained long-period "drift" or "trend" component of the input time series.

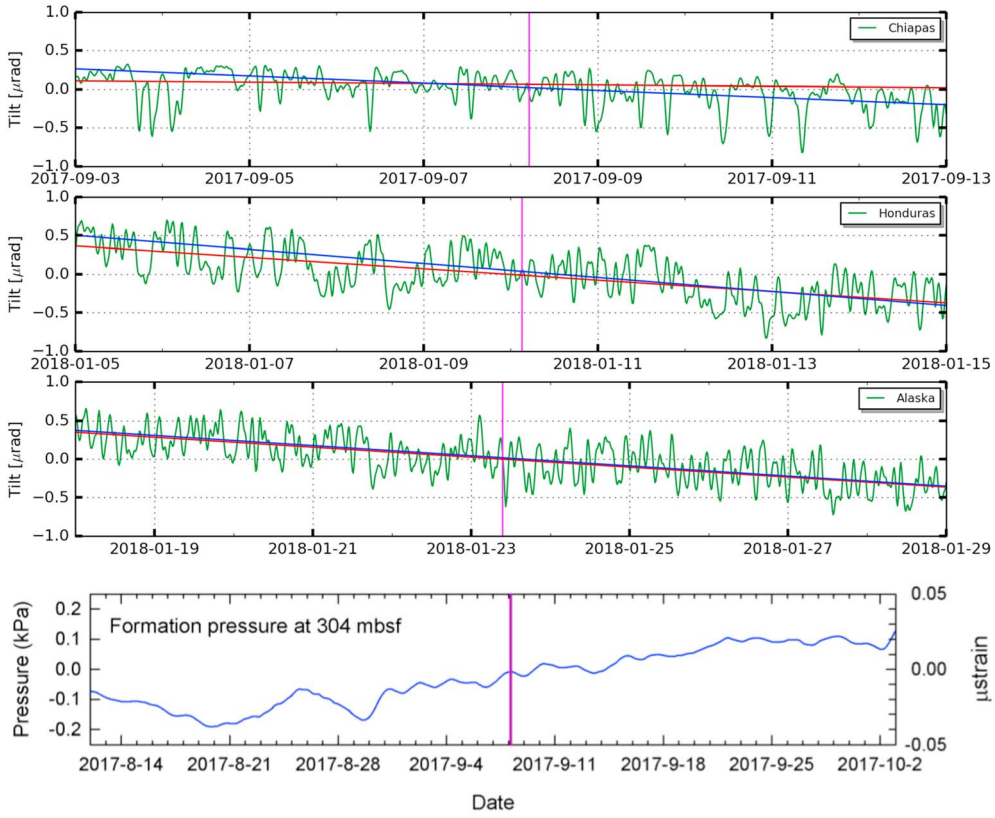

Figure 3. The top 3 panels show residual tilts for the updip-downdip direction (channel LA1_B2) at the Clayoquot slope borehole observatory in International Ocean Drilling Program hole U1364A for the Chiapas Mexico, Honduras, and Gulf of Alaska earthquakes. The vertical blue lines denote the time of the earthquake. For each earthquake, the tidal signal has been removed using a nonparametric Bayseian approach (Tamura et al., 1991). To determine if slow slip events were triggered by the passing surface waves, we fit a line to the 5 days before (red) and 5 days after (blue). In each case there is almost no measurable offset between the two lines at the time of the earthquake (<0.1 μR). This lack of measurable deformation does not depend on the de-tiding method (see Figure S2) or the exact definition of the before and after time periods. The bottom panel shows a representative formation pressure record spanning a 2-month period centered on the Chiapas earthquake. Seafloor pressure loading has been removed from the formation pressure record from 304 m below seafloor. The right-hand scale shows the magnitude of strain derived from formation pressure assuming a sensitivity of 0.5 kPa/μ strain (see Figure S3).

We used the unrotated data from one of the tilt sensors (SEED channel code LA1_B2, oriented at 225°), first down-sampling the 1 sample-per-second data to a sample interval of 15 min. De-tided residual signals shown in Figure 3 were calculated using continuous time series of lengths 135 days (top panel) and 117 days (bottom two panels).

We also examined the seafloor and 304-mbsf borehole pressure records for evidence of SSEs. Oceanographic signals preclude detection of vertical deformation with useful sensitivity, but the seafloor record can be used to eliminate loading effects from the formation records. In the example shown for the Chiapas earthquake in Figure 3, the formation pressure anomaly is computed by first determining the amplitude and phase of the formation tidal components relative to the seafloor record, then subtracting the scaled seafloor record from the formation record. The remaining tidal residuals associated with hydrologic diffusion and Earth tides are reduced by filtering. The resulting records show no transients greater than roughly 0.02–0.04 kPa, that is, less than the signal that would be expected from a M4 or M5 SSE (Figure 4). We also examined the seafloor pressure signal at 1364A recorded during the 2012 Haida Gwaii earthquake and found no resolvable seafloor deformation from that stress transient (Figures S1 and S4).

The de-tided tilt time series (Figure 3) also show no obvious signs of large transients either at the time of passing surface waves (e.g., similar to faults in California) or over the time scales of a few days afterwards

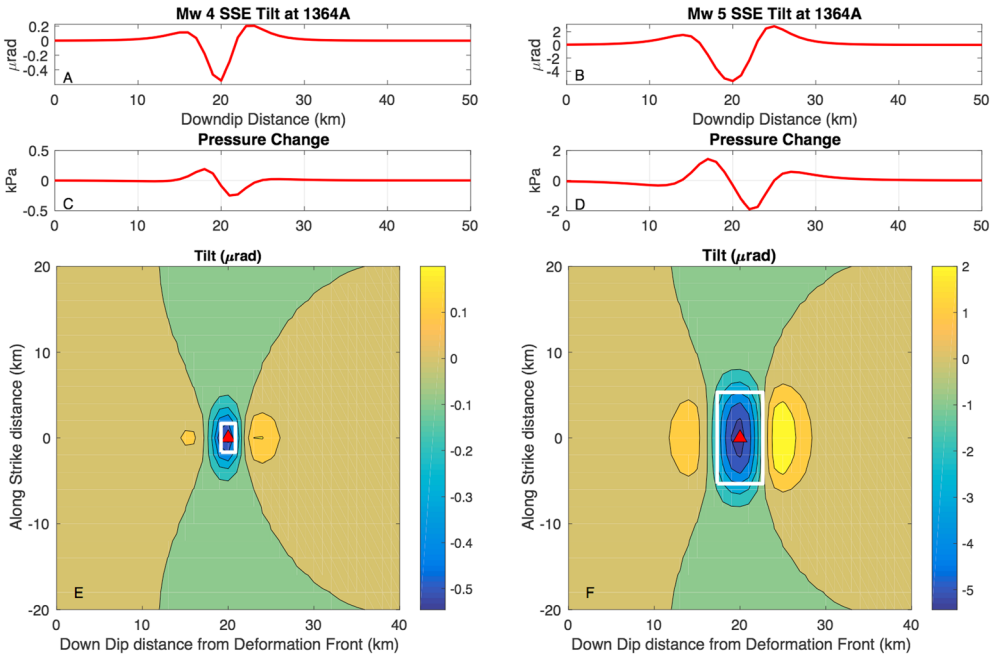

Figure 4. Expected signals from simple models of slow slip events (SSEs). (a and b) Predicted updip-downdip component of tilt and (c and d) pressure change at the borehole, for an M_w 4.0 and 5.0 SSE, respectively, as a function of distance from the deformation front. (e and f) SSEs are modeled as a rectangular rupture patch (white boxes in e and f, respectively) centered at the hole U1364A borehole location (red triangle in e and f) 20 km downdip from the deformation front. These profiles are taken through the borehole (0 km along strike distance in e and f). (e) and (f) show map views of the updip-downdip component of the tilt field. The color bars are tilt in microradians. If an M_w 4.0 event occurred within ~5 km of the borehole or an M_w 5.0 event occurred within about 10 km of the borehole, it would be detectable on the de-tided tilt and pressure records in Figure 3.

(e.g., similar to Nankai and Hikurangi). To quantify the lack of instantaneous triggered creep events similar to faults in California, we fit straight lines to the 5 days of data before each earthquake as well as to the 5 days after each earthquake and compared the offset at the time of the earthquake. In all three cases, any offsets at the time of the earthquake are constrained to be less than 0.1 μrad. Anomalies were also absent in the borehole pressure records, although the detection thresholds for pressure and volumetric strain are limited by the degree to which oceanographic loading effects can be removed, roughly 0.02 kPa and 0.05 μ strain, respectively (Figure 3).

We simulated the amplitude of the tilt and borehole pressure signals expected from triggered SSEs. To simulate SSEs that might be recorded at the U1364A observatory, we constructed a simple plate interface model shown in Figure S5 that mimics the constraints from active source refraction profiles (Yuan et al., 1994). We calculated tilt for SSEs located on this profile with simple Okada solutions (Okada, 1985) for a buried rectangular fault and assumed a Poisson ratio of 0.25. Hole U1364A is located ~20 km downdip of the deformation front. The SSEs are assumed to have a low value of stress drop, 0.1 MPa, similar to the Nankai and Hikurangi observations. The borehole pressure changes are calculated, assuming the pressure change is a linear function of volumetric strain with a coefficient of 4 kPa/microstrain.

The peak amplitude for an SSE immediately beneath the borehole would be 0.5 μrad and 0.2 kPa for an M_w 4.0 and 5 μrad and 2 kPa for an M_w 5.0 SSE (Figures 4 and S5), both of which are ruled out by Figure 3. If an event the size of the triggered Nankai (Araki et al., 2017; *M*5.5) or Hikurangi (Wallace et al., 2017; *M*7) SSEs had occurred within a few tens of km of the borehole, tilt and pressure signals would have been in the >10 μrad and >2-kPa range; hence, this scenario is ruled out by both the borehole tilt and pressure data. While the transient stresses observed at U1364A are smaller than those from large regional earthquakes in Nankai and Hikurangi, they are similar to some triggering examples from moderate (*M*5) regional events (Nakano et al., 2018; Araki et al., 2017) as well as some teleseismic examples (Zigone et al., 2012). Thus, the

response of the updip end of the Cascadia subduction zone offshore of Vancouver Island appears to be different compared to Nankai. It is also sufficiently different from the shallow parts of crustal strike-slip faults in California that occur within sedimentary basins (Wei et al., 2013), some of which underwent triggered slow slip from the Mexico earthquake's surface waves (M. Wei., pers. comm.). The complete absence of triggered tremor and SSEs at Clayoquot Slope, despite the ~10-kPa dynamic stress changes, likely implies that this portion of the fault has significantly different rheological properties and stress state than some other shallow megathrusts and crustal faults.

4. Discussion

One interpretation consistent with the lack of triggered updip tremor and SSEs is that the fault is locked in the vicinity of the Clayoquot Slope observatory during the current part of the inter-seismic period. It is likely that the updip frictional stability transition from aseismic (velocity strengthening) to seismic (velocity weakening) failure, in subduction zones with such a transition, is a gradual process owing to the large number of fault surfaces and potential mechanisms involved. Well instrumented subduction zones have shown an aseismic region near the trench where microearthquakes do not nucleate (Hirata et al., 1985; Suzuki et al., 2012). The transition from aseismic to seismogenic behavior has been suggested to correlate with the ~100–150 °C temperature range, which may indicate that the transition in clay mineralogy from smectite to illite is an important factor, although lab friction experiments have not always supported the idea that illite can sustain seismic rupture (Saffer et al., 2012; Saffer & Marone, 2003). Alternatively, the location of the 150 °C isotherm often corresponds to the region where a number of low-grade metamorphic processes lithify the overriding sediments and produce a rock sufficiently competent to support seismogenic stress levels (Moore & Saffer, 2001). In Cascadia, owing to the young age of the subducting plate and thick sediment cover, the thrust interface at the base of the accretionary prism is thought to have a temperature of about 160–200 °C near the deformation front (Gao & Wang, 2014; Hyndman & Wang, 1995; Salmi et al., 2017), which may rapidly warm to as high as 350 °C by 50 km downdip (Johnson et al., 2013), implying that the fault zone clay mineralogy is predominately illite. Recent experiments on illite-quartz mixtures have suggested that the upper stability transition on megathrust faults likely occurs at about 250 °C (den Hartog et al., 2012), leaving open the possibility of a small velocity strengthening region near the deformation front but likely indicating the fault should be dominated by velocity weakening friction beneath the U1364A borehole. Our observations are consistent with a view of the shallow part of the Cascadia megathrust offshore Vancouver Island operating at elevated temperatures and hence being locked most if not all the way to the deformation front.

An alternate view into the shallow locking state in Cascadia comes from models of past tsunamis. The height of the modeled tsunami when it reaches the shoreline in Cascadia can range from about 10 m for rupture scenarios with little slip near the deformation front to as much as 20 m for scenarios where slip peaks near the trench (Priest et al., 2009). At least for central Oregon, the geologic record of paleo-tsunami inundation distances appears most consistent with "buried" ruptures, where large slip does not extend to the trench (Priest et al., 2009). Similarly, observations of fold structures in the fore-arc offshore of Oregon suggest a transition from strong coupling under the Pliocene portion of the inner accretionary wedge to relatively little shear stress coupling in the Pleistocene wedge near the deformation front (Goldfinger et al., 1992). Recent seismic imaging studies have inferred a variation in the locking state between the relatively uncoupled region offshore of Oregon and the more strongly coupled region to the north offshore of Washington that results from variations in sediment consolidation (Han et al., 2017) and increasing temperature. Our results would be consistent with the strongly coupled zone extending farther north to central Vancouver Island. To fully constrain the interseismic frictional properties of the Cascadia megathrust, a widespread network of continuous seafloor geodetic observations is needed. Highly sensitive borehole observatories similar to the Clayoquot Slope observatory would be particularly useful in regions where the thrust interface routinely undergoes stress transients due to intraplate faulting within the subducting slab (Gong & McGuire, 2018) or due to the adjacent Nootka fault zone, the seismically active transform boundary between the Juan de Fuca and Explorer plates that lies 100 km northwest of the hole U1364A observatory. The ability of larger dynamic stress transients than those studied here to trigger SSEs on the thrust interface offshore of Vancouver Island will likely be evaluated in the future using large ($M > 6.5$) events on the nearby Nootka Fault zone and possibly other regional earthquakes.

Acknowledgments
We thank the W. M. Keck Foundation for funding the construction of the seismic and geodetic observatory system. We thank J. O'Brien and K. von der Heydt for their work designing, constructing, testing, and installing the borehole instrumentation. We thank D. Kot, J. Ryder, and Ian Kulin for their work on the deployment cruise. We thank the crew of the R/V *Sikuliaq* and the ROV Jason team for performing the installation of the borehole instrumentation. K. Becker was supported by NSF grant OCE-1259718. McGuire and Collins were supported by NSF grant OCE-1259243. Drilling of Hole U1364A and installation of the ACORK infrastructure was carried out by the Integrated Ocean Drilling Program, and support for the pressure monitoring instrumentation was provided by Ocean Networks Canada and the Geological Survey of Canada. We thank Noel Bartlow and Laura Wallace for helpful reviews. Data Statement All data for this project are archived at the Ocean Networks Canada (ONC) and IRIS data centers.

References

Araki, E., Saffer, D. M., Kopf, A. J., Wallace, L. M., Kimura, T., Machida, Y., et al., & I. E. 3. S. scientists (2017). Recurring and triggered slow-slip events near the trench at the Nankai trough subduction megathrust. *Science*, *356*(6343), 1157–1160. https://doi.org/10.1126/science.aan3120

Atwater, B. F. (1987). Evidence for great Holocene earthquakes along the outer coast of Washington state. *Science*, *236*(4804), 942–944. https://doi.org/10.1126/science.236.4804.942

Bilham, R. (1989). Surface slip subsequent to the 24 November 1987 Superstition Hills, California, earthquake monitored by digital creepmeters. *Bulletin of the Seismological Society of America*, *79*(2), 424–450.

Briggs, R. W., Sieh, K., Meltzner, A. J., Natawidjaja, D., Galetzka, J., Suwargadi, B., et al. (2006). Deformation and slip along the Sunda megathrust in the great 2005 Nias-Simeulue earthquake. *Science*, *311*(5769), 1897–1901. https://doi.org/10.1126/science.1122602

Brown, K., Tryon, M., Deshon, H., Dorman, L., & Schwartz, S. (2005). Correlated transient fluid pulsing and seismic tremor in the Costa Rica subduction zone. *Earth and Planetary Science Letters*, *238*(1–2), 189–203. https://doi.org/10.1016/j.epsl.2005.06.055

Cattania, C., McGuire, J. J., & Collins, J. A. (2017). Dynamic triggering and earthquake swarms on East Pacific Rise transform faults. *Geophysical Research Letters*, *44*, 702–710. https://doi.org/10.1002/2016GL070857

Collins, J. A., McGuire, J. J., & Wei, M. (2013). Shear-wave velocity structure and inter-seismic strain accumulation in the up-dip region of the Cascadia subduction zone: Similarities to Tohoku? AGU Fall Meeting Abstracts.

Davis, E., Kinoshita, M., Becker, K., Wang, K., Asano, Y., & Ito, Y. (2013). Episodic deformation and inferred slow slip at the Nankai subduction zone during the first decade of CORK borehole pressure and VLFE monitoring. *Earth and Planetary Science Letters*, *368*, 110–118. https://doi.org/10.1016/j.epsl.2013.03.009

Davis, E. E., Malone, M. J., & Expedition 328 Scientists and Engineers (2010). *Cascadia subduction zone ACORK observatory, IODP Prel. Rept., 328*. https://doi.org/10.2204/iodp.pr.328.2010

Davis, E. E., Villinger, H., & Sun, T. (2015). Slow and delayed deformation and uplift of the outermost subduction prism following ETS and seismogenic slip events beneath Nicoya Peninsula, Costa Rica. *Earth and Planetary Science Letters*, *410*, 117–127. https://doi.org/10.1016/j.epsl.2014.11.015

den Hartog, S. A. M., Peach, C. J., de Winter, D. A. M., Spiers, C. J., & Shimamoto, T. (2012). Frictional properties of megathrust fault gouges at low sliding velocities: New data on effects of normal stress and temperature. *Journal of Structural Geology*, *38*(C), 156–171. https://doi.org/10.1016/j.jsg.2011.12.001

Dixon, T. H., Jiang, Y., Malservisi, R., McCaffrey, R., Voss, N., Protti, M., & Gonzalez, V. (2014). Earthquake and tsunami forecasts: Relation of slow slip events to subsequent earthquake rupture. *Proceedings of the National Academy of Sciences of the United States of America*, *111*(48), 17,039–17,044. https://doi.org/10.1073/pnas.1412299111

Duputel, Z., Jiang, J., Jolivet, R., Simons, M., Rivera, L., Ampuero, J. P., et al. (2015). The Iquique earthquake sequence of April 2014: Bayesian modeling accounting for prediction uncertainty. *Geophysical Research Letters*, *42*, 7949–7957. https://doi.org/10.1002/2015GL065402

Gagnon, K., Chadwell, C. D., & Norabuena, E. (2005). Measuring the onset of locking in the Peru-Chile trench with GPS and acoustic measurements. *Nature*, *434*(7030), 205–208. https://doi.org/10.1038/nature03412

Gao, X., & Wang, K. (2014). Strength of stick-slip and creeping subduction megathrusts from heat flow observations. *Science*, *345*(6200), 1038–1041. https://doi.org/10.1126/science.1255487

Goldfinger, C., Kulm, L. D., Yeats, R. S., Appelgate, B., MacKay, M. E., & Moore, G. F. (1992). Transverse structural trends along the Oregon convergent margin: Implications for Cascadia earthquake potential and crustal rotations. *Geology*, *20*(2), 141–144. https://doi.org/10.1130/0091-7613(1992)020<0141:TSTATO>2.3.CO;2

Goldfinger, C., Nelson, C. H., Morey, A. E., Johnson, J. E., Patton, J. R., Karabanov, E., et al. (2012). Turbidite event history—Methods and implications for Holocene paleoseismicity of the Cascadia subduction zone: U.S. Geological Survey Professional Paper 1661–F (170 pp.). Retrieved from https://pubs.usgs.gov/pp/pp1661f/

Gong, J., & McGuire, J. J. (2018). Interactions between strike-slip earthquakes and the subduction interface near the Mendocino triple junction. *Earth and Planetary Science Letters*, *482*, 414–422. https://doi.org/10.1016/j.epsl.2017.11.022

Han, S., Bangs, N. L., Carbotte, S. M., Saffer, D. M., & Gibson, J. C. (2017). Links between sediment consolidation and Cascadia megathrust slip behaviour. *Nature Geoscience*, *10*(12), 954–959. https://doi.org/10.1038/s41561-017-0007-2

Hirata, N., Kanazawa, T., Suehiro, K., & Shimamura, H. (1985). A seismicity gap beneath the inner wall of the Japan trench as derived by ocean bottom seismography measurement. *Tectonophysics*, *112*(1-4), 193–209. https://doi.org/10.1016/0040-1951(85)90179-9

Hyndman, R. D., & Wang, K. (1995). The rupture zone of Cascadia great earthquakes from current deformation and the thermal regime. *Journal of Geophysical Research*, *100*(B11), 22,133–22,154. https://doi.org/10.1029/95JB01970

Hyndman, R. D., Wang, K., Yuan, T., & Spence, G. D. (1993). Tectonic sediment thickening, fluid expulsion, and the thermal regime of subduction zone accretionary prisms: The Cascadia margin off Vancouver Island. *Journal of Geophysical Research*, *98*(B12), 21,865–21,876.

Iinuma, T., Hino, R., Kido, M., Inazu, D., Osada, Y., Ito, Y., et al. (2012). Coseismic slip distribution of the 2011 off the Pacific Coast of Tohoku earthquake (M9.0) refined by means of seafloor geodetic data. *Journal of Geophysical Research*, *117*, B07409. https://doi.org/10.1029/2012JB009186

Itaba, S., & Ando, R. (2011). A slow slip event triggered by teleseismic surface waves. *Geophysical Research Letters*, *38*, L21306. https://doi.org/10.1029/2011GL049593

Johnson, H. P., Solomon, E. A., Harris, R. N., Salmi, M. S., & Berg, R. D. (2013). Heat flow and fluid flux in Cascadia's seismogenic zone. *Eos, Transactions of the American Geophysical Union*, *94*(48), 457–458. https://doi.org/10.1002/2013EO480001

Kaneko, Y., & Fialko, Y. (2011). Shallow slip deficit due to large strike-slip earthquakes in dynamic rupture simulations with elasto-plastic off-fault response. *Geophysical Journal International*, *186*(3), 1389–1403. https://doi.org/10.1111/j.1365-246X.2011.05117.x

McCrory, P. A., Blair, J. L., Waldhauser, F., & Oppenheimer, D. H. (2012). Juan de Fuca slab geometry and its relation to Wadati-Benioff zone seismicity. *Journal of Geophysical Research*, *117*, B09306. https://doi.org/10.1029/2012JB009407

Miyazawa, M., & Brodsky, E. E. (2008). Deep low-frequency tremor that correlates with passing surface waves. *Journal of Geophysical Research*, *113*, B04302. https://doi.org/10.1029/2006JB004890

Moore, J. C., & Saffer, D. (2001). Updip limit of the seismogenic zone beneath the accretionary prism of southwest Japan: An effect of diagenetic to low-grade metamorphic processes and increasing effective stress. *Geology*, *29*(2), 183–186. https://doi.org/10.1130/0091-7613(2001)029<0183:ULOTSZ>2.0.CO;2

Nakamura, M., & Sunagawa, N. (2015). Activation of very low frequency earthquakes by slow slip events in the Ryukyu trench. *Geophysical Research Letters*, *42*, 1076–1082. https://doi.org/10.1002/2014GL062929

Nakano, M., Hori, T., Araki, E., Kodaira, S., & Ide, S. (2018). Shallow very-low-frequency earthquakes accompany slow slip events in the Nankai subduction zone. *Nature Communications*, *9*(1), 984. https://doi.org/10.1038/s41467-018-03431-5

Obara, K., & Ito, Y. (2005). Very low frequency earthquakes excited by the 2004 off the Kii peninsula earthquakes: A dynamic deformation process in the large accretionary prism. *Earth, Planets and Space*, *57*(4), 321–326. https://doi.org/10.1186/BF03352570

Obara, K., & Kato, A. (2016). Connecting slow earthquakes to huge earthquakes. *Science*, *353*(6296), 253–257. https://doi.org/10.1126/science.aaf1512

Okada, Y. (1985). Surface deformation due to shear and tensile faults in a half-space. *Bulletin of the Seismological Society of America*, *75*(4), 1135–1154.

Peng, Z., & Gomberg, J. (2010). An integrated perspective of the continuum between earthquakes and slow-slip phenomena. *Nature Geoscience*, *3*(9), 599–607. https://doi.org/10.1038/ngeo940

Pollitz, F. F., & Evans, E. L. (2017). Implications of the earthquake cycle for inferring fault locking on the Cascadia megathrust. *Geophysical Journal International*, 167–185. https://doi.org/10.1093/gji/ggx009

Priest, G. R., Goldfinger, C., Wang, K., Witter, R. C., Zhang, Y., & Baptista, A. M. (2009). Confidence levels for tsunami-inundation limits in northern Oregon inferred from a 10,000-year history of great earthquakes at the Cascadia subduction zone. *Natural Hazards*, *54*(1), 27–73. https://doi.org/10.1007/s11069-009-9453-5

Rubinstein, J. L., Gomberg, J., Vidale, J. E., Wech, A. G., Kao, H., Creager, K. C., & Rogers, G. (2009). Seismic wave triggering of nonvolcanic tremor, episodic tremor and slip, and earthquakes on Vancouver Island. *Journal of Geophysical Research*, *114*, B00A01. https://doi.org/10.1029/2008JB005875

Rubinstein, J. L., Vidale, J. E., Gomberg, J., Bodin, P., Creager, K. C., & Malone, S. D. (2007). Non-volcanic tremor driven by large transient shear stresses. *Nature*, *448*(7153), 579–582. https://doi.org/10.1038/nature06017

Rymer, M. J., Treiman, J. A., Kendrick, K. J., Lienkaemper, J. J., Weldon, R. J., Bilham, R., et al. (2011). Triggered surface slips in southern California associated with the 2010 El Mayor-Cucapah, Baja California, Mexico, earthquake, USGS Open-File Report.

Saffer, D. M., Lockner, D. A., & McKiernan, A. (2012). Effects of smectite to illite transformation on the frictional strength and sliding stability of intact marine mudstones. *Geophysical Research Letters*, *39*, L11304. https://doi.org/10.1029/2012GL051761

Saffer, D. M., & Marone, C. (2003). Comparison of smectite- and illite-rich gouge frictional properties: Application to the updip limit of the seismogenic zone along subduction megathrusts. *Earth and Planetary Science Letters*, *215*(1–2), 219–235. https://doi.org/10.1016/S0012-821X(03)00424-2

Salmi, M. S., Johnson, H. P., & Harris, R. N. (2017). Thermal environment of the southern Washington region of the Cascadia subduction zone. *Journal of Geophysical Research: Solid Earth*, *122*, 5852–5870. https://doi.org/10.1002/2016JB013839

Schmalzle, G. M., McCaffrey, R., & Creager, K. C. (2014). Central Cascadia subduction zone creep. *Geochemistry, Geophysics, Geosystems*, *15*, 1515–1532. https://doi.org/10.1002/2013GC005172

Sun, T., Davis, E. E., Wang, K., & Jiang, Y. (2017). Trench-breaching afterslip following deeper coseismic slip of the 2012 Mw 7.6 Costa Rica earthquake constrained by near-trench pressure and land-based geodetic observations. *Earth and Planetary Science Letters*, *479*, 263–272. https://doi.org/10.1016/j.epsl.2017.09.021

Sun, T., Fujiwara, T., Kodaira, S., He, J., & Wang, K. (2017). Large fault slip peaking at trench in the 2011 Tohoku-oki earthquake. *Nature Communications*, *8*, 1–8. https://doi.org/10.1038/ncomms14044

Suzuki, K., Hino, R., Ito, Y., Yamamoto, Y., Suzuki, S., Fujimoto, H., et al. (2012). Seismicity near the hypocenter of the 2011 of the Pacific coast of Tohoku earthquake deduced by using ocean bottom seismographic data. *Earth, Planets and Space*, *64*(12), 1125–1135. https://doi.org/10.5047/eps.2012.04.010

Tamura, Y., Sato, T., Ooe, M., & Ishiguro, M. (1991). A procedure for tidal analysis with a Bayesian information criterion. *Geophysical Journal International*, *104*(3), 507–516. https://doi.org/10.1111/j.1365-246X.1991.tb05697.x

To, A., Obana, K., Sugioka, H., Araki, E., Takahashi, N., & Fukao, Y. (2015). Small size very low frequency earthquakes in the Nankai accretionary prism, following the 2011 Tohoku-Oki earthquake. *Physics of the Earth and Planetary Interiors*, *245*, 40–51. https://doi.org/10.1016/j.pepi.2015.04.007

Tromp, J., Komatitsch, D., Hjörleifsdóttir, V., Liu, Q., Zhu, H., Peter, D., et al. (2010). Near real-time simulations of global CMT earthquakes. *Geophysical Journal International*, *183*(1), 381–389. https://doi.org/10.1111/j.1365-246X.2010.04734.x

Wallace, L. M., Kaneko, Y., Hreinsdóttir, S., Hamling, I., Peng, Z., Bartlow, N., et al. (2017). Large-scale dynamic triggering of shallow slow slip enhanced by overlying sedimentary wedge. *Nature Geoscience*, *10*(10), 765–770. https://doi.org/10.1038/ngeo3021

Wallace, L. M., Webb, S. C., Ito, Y., Mochizuki, K., Hino, R., Henrys, S., et al. (2016). Slow slip near the trench at the Hikurangi subduction zone, New Zealand. *Science*, *352*(6286), 701–704. https://doi.org/10.1126/science.aaf2349

Walter, J. I., Schwartz, S. Y., Protti, M., & Gonzalez, V. (2013). The synchronous occurrence of shallow tremor and very low frequency earthquakes offshore of the Nicoya Peninsula, Costa Rica. *Geophysical Research Letters*, *40*, 1517–1522. https://doi.org/10.1002/grl.50213

Wang, K., & Tréhu, A. M. (2016). Invited review paper: Some outstanding issues in the study of great megathrust earthquakes—The Cascadia example. *Journal of Geodynamics*, *98*, 1–18. https://doi.org/10.1016/j.jog.2016.03.010

Wei, M., Kaneko, Y., Liu, Y., & McGuire, J. J. (2013). Episodic fault creep events in California controlled by shallow frictional heterogeneity. *Nature Geoscience*, *6*(7), 566–570. https://doi.org/10.1038/ngeo1835

Wei, M., Kaneko, Y., Shi, P., & Liu, Y. (2018). Numerical modeling of dynamically triggered shallow slow slip events in New Zealand by the 2016 Mw 7.8 Kaikoura earthquake. *Geophysical Research Letters*, *119*(6343), 6992. https://doi.org/10.1029/2018GL077879

Wei, M., Liu, Y., Kaneko, Y., McGuire, J. J., & Bilham, R. (2015). Dynamic triggering of creep events in the Salton trough, Southern California by regional M≥5.4 earthquakes constrained by geodetic observations and numerical simulations. *Earth and Planetary Science Letters*, *427*(C), 1–10. https://doi.org/10.1016/j.epsl.2015.06.044

Wei, M., Sandwell, D., Fialko, Y., & Bilham, R. (2011). Slip on faults in the Imperial Valley triggered by the 4 April 2010 Mw 7.2 El Mayor-Cucapah earthquake revealed by InSAR. *Geophysical Research Letters*, *38*, L01308. https://doi.org/10.1029/2010GL045235

Wilcock, W. S. D., Stafford, K. M., Andrew, R. K., & Odom, R. I. (2014). Sounds in the Ocean at 1–100 Hz, *Annual Review of Marine Science*, *6*(1), 117–140. https://doi.org/10.1146/annurev-marine-121211-172423

Yokota, Y., Ishikawa, T., Watanabe, S.-I., Tashiro, T., & Asada, A. (2016). Seafloor geodetic constraints on interplate coupling of the Nankai trough megathrust zone. *Nature*, *534*(7607), 374–377. https://doi.org/10.1038/nature17632

Yuan, T., Spence, G. D., & Hyndman, R. D. (1994). Seismic velocities and inferred porosities in the accretionary wedge sediments at the Cascadia margin. *Journal of Geophysical Research*, *99*(B3), 4413–4427. https://doi.org/10.1029/93JB03203

Zigone, D., Rivet, D., Radiguet, M., Campillo, M., Voisin, C., Cotte, N., et al. (2012). Triggering of tremors and slow slip event in Guerrero, Mexico, by the 2010 Mw 8.8 Maule, Chile, earthquake. *Journal of Geophysical Research*, *117*, B09304. https://doi.org/10.1029/2012JB009160